

# NAVAL POSTGRADUATE SCHOOL

## Monterey, California



MARINE ATMOSPHERIC BOUNDARY LAYER  
MODELING FOR TACTICAL USE

K. L. Davidson, G. E. Schacher, C. W. Fairall,  
P. Jones Boyle and D. A. Brower

September 1982

Technical Report:                      October 1981 to October 1982

Approved for public release; distribution unlimited.

Prepared for: Naval Air Systems Command  
AIR 370  
Washington, DC 20360

FedDocs  
D 208.14/2  
NPS-63-82-001

FORM 100-101  
100-101  
NPS-101-101-101

NAVAL POSTGRADUATE SCHOOL  
Monterey, California 93940

Rear Admiral J. J. Ekelund  
Superintendent

D. A. Schraday  
Provost

The work reported herein has been supported by NAVAIR (AIR-370), NAVMAT (Navy EOMET), and NAVSEA (PMS-405).

Reproduction of all or part of this report is authorized.

This report was prepared by:

SECURITY CLASSIFICATION OF THIS PAGE (When Data Entered)

REPORT DOCUMENTATION PAGE		READ INSTRUCTIONS BEFORE COMPLETING FORM
1. REPORT NUMBER NPS63-82-001	2. GOVT ACCESSION NO.	3. RECIPIENT'S CATALOG NUMBER
4. TITLE (and Subtitle) Marine Atmospheric Boundary Layer Modeling for Tactical Use		5. TYPE OF REPORT & PERIOD COVERED Technical Report October 1981 - October 1982
		6. PERFORMING ORG. REPORT NUMBER
7. AUTHOR(s) K. L. Davidson, G. E. Schacher, C. W. Fairall, P. Jones Boyle and D. A. Brower		8. CONTRACT OR GRANT NUMBER(s)
9. PERFORMING ORGANIZATION NAME AND ADDRESS Naval Postgraduate School Monterey, California 93940		10. PROGRAM ELEMENT, PROJECT, TASK AREA & WORK UNIT NUMBERS
11. CONTROLLING OFFICE NAME AND ADDRESS Naval Air Systems Command Code AIR-370 Washington, DC 20360		12. REPORT DATE
		13. NUMBER OF PAGES
14. MONITORING AGENCY NAME & ADDRESS (if different from Controlling Office)		15. SECURITY CLASS. (of this report)  Unclassified
		15a. DECLASSIFICATION/DOWNGRADING SCHEDULE
16. DISTRIBUTION STATEMENT (of this Report)  Approved for public release; distribution unlimited.		
17. DISTRIBUTION STATEMENT (of the abstract entered in Block 20, if different from Report)		
18. SUPPLEMENTARY NOTES  * C. W. Fairall is a contract employee with BDM Corporation.		
19. KEY WORDS (Continue on reverse side if necessary and identify by block number)  Marine Boundary Layer, Boundary Layer Modeling, Tactical Aids		
20. ABSTRACT (Continue on reverse side if necessary and identify by block number)  The properties of the lower atmosphere are very important in the operation of many systems. Of particular importance is the effect on electromagnetic propagation for the full range from optical to radio wavelengths. Small scale fluctuations and aerosols severely affect optical propagation. Large scale changes in the index of refraction cause bending of rf and microwaves, leading to ducting, fading, and a host of other phenomena. Experimental assessment of atmospheric properties can only be done occasionally and on a widely		

separated basis. Thus, it is critical for operational planning to have available a model which can extend routine atmospheric measurements (radiosonde) in both time and space. At NPS extensive work is underway on modeling the marine atmospheric boundary layer. We sketch here the basics of the model and describe how it can be used to provide the needed inputs for tactical models.

## TABLE OF CONTENTS

1.	INTRODUCTION - - - - -	7
2.	ATMOSPHERIC MODELING FOR TACTICAL DESCRIPTIONS - - - - -	10
3.	ATMOSPHERIC BOUNDARY LAYER MODEL CONSIDERATIONS - - - - -	19
4.	MODELING THE BOUNDARY LAYER - - - - -	22
5.	MODEL VALIDATION - - - - -	28
	A. DATA SET - - - - -	28
	B. OBSERVED CHANGES - - - - -	30
	C. MODEL PREDICTIONS - - - - -	31
6.	CONCLUSIONS - - - - -	40
	REFERENCES - - - - -	43
	DISTRIBUTION LIST - - - - -	44

## LIST OF FIGURES

- Figure 1. Simplified flow diagram of the boundary layer model showing possible configurations of input information, interrelation between atmospheric and oceanic models, model outputs, and tactical models which use these outputs.
- Figure 2. Examples of extended ranges and holes for EM ducts for (a) surface-based duct and a shipboard air-search radar and (b) elevated duct and an airborne early-warning radar (from Hitney, 1979).
- Figure 3. Computer simulated image remotely piloted vehicle (RPV) as viewed with 8-12  $\mu\text{m}$  IR sensor (range 2 km, visibility 15 km, threshold 4.5 nW) through atmosphere with  $C_n^2$  values of (a) 0 (no turbulence), (b)  $3.7 \times 10^{-15} \text{ m}^{-2/3}$  and (c)  $1.0 \times 10^{-14} \text{ m}^{-2/3}$  (from Kearns and Walter, 1978).
- Figure 4. Measured variation of  $C_n^2$  with height. Data were obtained during the CEWCOM-76 experiment, 5 Oct 76.
- Figure 5. Variation of laser beam radius with distance for  $C_n^2$  levels of  $6.5 \times 10^{-5} \text{ m}^{-2/3}$  (solid line) and  $6.5 \times 10^{-13} \text{ m}^{-2/3}$  (dashed line).
- Figure 6. Idealized profiles of virtual potential temperature,  $\theta_v$ , and water vapor mixing ratio,  $Q$ , in a mixed-layer atmosphere.
- Figure 7. Schematic input, prescription and computing steps in MABL prediction.
- Figure 8. Track of R/V ACANIA and location of shoreline radiosonde sites during CEWCOM-78. The general location of the R/V ACANIA during the 19-21 May period is indicated by the hatched area N-NW of San Nicolas Island (SNI).



- Figure 9. Atmospheric and oceanic mixed-layer observations during CEWCOM-78; (a) potential temperature composite profiles, (b) acoustic sounder record, (c) 10 meter relative humidity, (d) 10 meter and sea surface temperatures, (e) 10 meter wind speed. All data except the profiles indicated in (a) were obtained from the R/V ACANIA.
- Figure 10. Observed profiles of the modified refractivity,  $M$ . Data were obtained at the approximate times indicated. The dotted line shows the boundary of the radar duct.
- Figure 11. Observed and predicted MABL profiles for the 5/19/0500 to 5/21/0500 CEWCOM-78 period including (a)  $Q$  ( $\text{gm}^{-3}$ ) and  $\theta$  ( $^{\circ}\text{C}$ ), (b)  $M$ , (c)  $C_n^2$  ( $\text{m}^{-2/3}$ ), and (d) total extinction coefficient,  $\beta$  ( $\text{km}^{-1}$ ). Solid lines correspond to observations and dashed lines to model predicted values. The observed values were calculated from the meteorological parameters measured at the times indicated.
- Figure 12. Observed and predicted surface layer values for the 5/19/0500 to 5/21/0500 CEWCOM-78 period: (a) inversion height ( $Z_i$ ) (solid line) and lifting condensation level ( $Z_{lcl}$ ) (dotted line). The A's represent inversion height determined from radiosonde soundings taken on the R/V ACANIA, the X's are inversion heights from composite soundings. The O's represent corresponding observed  $Z_{lcl}$ 's. (b) evaporation duct depth,  $Z_e$  (m), (c)  $C_n^2$  ( $\text{m}^{-2/3}$ ), and (d) total aerosol and water vapor) scattering extinction coefficient,  $\beta$  ( $\text{km}^{-1}$ ). In (b)-(d) X's are the observed and solid lines are the model predicted values.

## ACKNOWLEDGMENTS

This work has been supported by several sponsors. They are NAVAIR (AIR-370) for the basic modeling effort, NAVMAT (Navy EOMET) for aerosol modeling and measurements, and NAVSEA (PMS-405) for optical turbulence interpretation. The valuable assistance of several people has aided this work, principally Dr. A. Goroch (NEPRF), Prof. J. Businger (U. of Washington) and Dr. B. Katz (NSWC, White Oak).



## 1. INTRODUCTION

This report describes the Naval Postgraduate School (NPS) Environmental Physics Group's approach to predicting properties of the marine atmospheric boundary layer which affect weapons systems. We describe tactically significant parameters and how they can be predicted using a boundary layer model. We also describe verification of the model with data gathered from shipboard sensors. This is the second in a series of reports on the NPS marine atmospheric prediction model; the first report was a position paper on the modeling method (Fairall et al, 1981).

Modern warfare has become critically dependent on nearly the entire electromagnetic spectrum for command, control and communications for weapon guidance, for electronic warfare support and for countermeasures. Thus, environmental enhancement or degradation of the performance of electromagnetic (EM) and electro-optic (EO) systems has become a primary concern of task force commanders. Tactically essential systems are affected by the environment even when meteorological conditions are not severe in the historical sense. The deployment of systems and the modification of tactics based on environmental factors will, to a large extent, determine the effectiveness of EM/EO sensor, weapon and communication systems.

The assessment of environmental effects on EM/EO systems is not a simple task because there are many variables to consider. A given platform may have many systems, each with its individual characteristics and purpose, and performance depends on such systems parameters as frequency, power, antenna gain and on such meteorological and oceanic parameters as wind speed, humidity, temperature and sea state. If a complete and accurate set of parameters describing the environment is available, the environmental impact on weapon systems can usually be calculated. However, the task force commander often

has an incomplete set of environmental parameters available to him and in a wartime situation his communication with external sources of information, such as Fleet Numerical Oceanography Center, may even be cut. It is therefore necessary for task force, or even individual ship commanders to be able to make spatial and temporal extrapolations of environmental parameters based solely on information they themselves can obtain and computational capabilities that reside with them.

A gap has existed in past efforts to characterize tactical environmental conditions. The gap was between the two extreme approaches of relating conditions to 1) near surface observations, and to 2) larger scale predicted synoptic patterns. Clearly, to assess the local features, local measurement is desirable. However, to assess over a large spatial region or for a long time period, a local measurement made at one time loses its validity. Thus, one must consider a transition to climatology, or large scale numerical analysis predictions, or dynamic models based on observations at the operational location. Climatologies do not include the small scale structure descriptions needed. Ruggles (1975) has examined the capabilities of large scale numerical procedures at remote facilities and argued convincingly that they are not sufficient for all tactical descriptions. Thus, we must rely on dynamic models that utilize both local measurements and large scale numerical predictions. This is the philosophy behind the Tactical Environmental Support System (TESS) concept and the NPS model we describe here.

Three types of models are needed to predict weapon system behavior. One is needed to calculate system performance given a set of environmental parameters. An example is the Integrated Refractive Effects Prediction System (IREPS) which determines and displays parameters affecting radar and communication systems using mean meteorological parameters as input information.

Another is required to calculate environmental parameters from readily available meteorological data. An example is the estimation of thermal turbulence needed to assess optical system performance, which cannot be measured directly but can be determined from radiosonde data. Finally, another is needed to predict the changes in the meteorological properties.

It is assumed at the outset that models should be developed which depend as much as possible on "single station assessments". That is, they should only require data which can be gathered from a single ship or station. The models should also have the capability to use data from many sources, which would improve the accuracy of the assessment, but multi-source data would not be a necessity. Another requirement is that it should be possible to run the model on a microcomputer, which would make it available to a wide range of users and compatible with the microcomputer based IREPS program.

## 2. ATMOSPHERIC MODELING FOR TACTICAL DESCRIPTIONS

Predicting the effect of the environment on tactical systems ranges from determining large scale atmospheric forcing on the boundary layer to assessment of the behavior of an actual system. The latter requires the placement of a set of instructions in the hands of the systems operator. This section describes the requirements on a boundary layer model, which is to be used to predict changes in significant propagation parameters within the first kilometer. The various models and their purposes within the tactical situation are tested in Table 1. The boundary layer model is only one of the models; it calculates the expected evolution of the boundary layer properties and outputs this information for use by propagation models.

A simplified schematic of the information flow between the models for environmental assessment is shown in Figure 1. The predicted properties would be used by such assessment systems as IREPS for radar and radio propagation, LOWTRAN and SAEL for optical propagation. The latter are shown on the RHS of Figure 1.

The two primary properties in the assessment of electromagnetic propagation are the index of refraction and extinction parameters.

Extinction: Extinction depends on the electromagnetic wavelength. In the radio and radar region extinction is due to scattering by droplets and from the sea surface and, to a lesser extent, scattering from refractive index inhomogeneities. In general, scattering is a minor effect on radio and radar frequencies for most cases except rain and high sea state surface. In the optical region, extinction is due to molecular absorption and aerosol scattering and can be quite severe. Molecular absorption occurs over narrow wavelength bands so that optical "windows" exist. Extinction in fog and clouds is so severe that most optical systems cannot be used.

Refraction: Index of refraction gradients exist over scales from kilometers to centimeters. Gradients over the large scale lead to ray path curvature which seriously affects the performance of radio and radar systems, but not optical systems which normally are operated over short paths. However, small scale index variations (1 cm to 10 m) can cause significant degradation in optical images and the energy density that can be obtained in an optical beam.

The tactical importance of variations in index of refraction gradients and variations is illustrated in Figures 2 and 3. Figure 2 illustrates refractive effects on the radar propagation index when the ray curvature is greater than the curvature of the earth. Figure 2a is for a surface based radar and 2b is for an airborne radar. Degradation of an optical image with increasing small scale index of refraction turbulence, in terms of the index of refraction structure function  $C_n^2$ , is shown in Figure 3. Values range from no turbulence, Figure 3a, to moderate turbulence, Figure 3c. As the figures indicate, atmospheric effects are of serious concern if effects such as those shown occur a significant fraction of the time.

Variation of  $C_n^2$  with height is shown in Figure 4. These data were obtained in an NPS experiment and are typical of what is observed in and at the top of a well mixed boundary layer.  $C_n^2$  is large near the surface and inversion. Reference to Figure 2 shows that values observed at the inversion lead to substantial degradation of optical images.

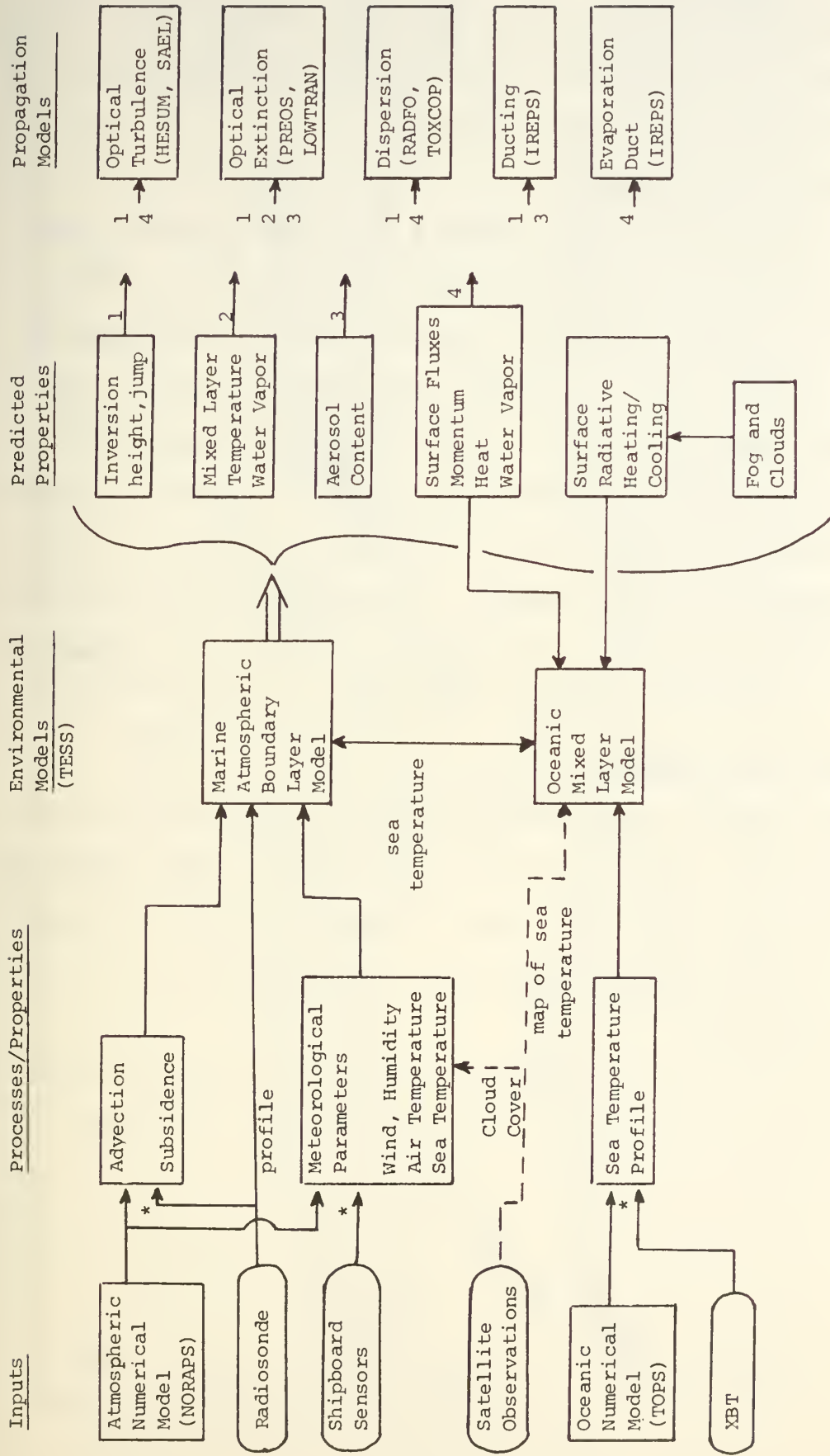
Beam spread with distance is shown in Figure 5 for  $C_n^2$  ranging from low to moderate values. For the lower turbulence value the beam radius increases by a factor of 4 from 1 km to 4 km, which corresponds to an order of magnitude decrease in energy density.



TABLE 1. Prediction/assessments and models required.

<u>Purpose</u>	<u>Required</u>	<u>Model type</u>
Synoptic Scale Forcing Winds	Subsidence Advection	Synoptic Scale Numerical
Local Meteorological Parameters	Inversion Temperature Humidity Clouds Winds	Boundary Layer
Propagation Parameters	Index of Refraction Aerosol Absorbing Molecules	Boundary Layer
EM/EO Behavior	Ray Curvature Visibility Image Resolution	System Dependent Propagation
Tactical Decision Aids	System Utilization Flight Pattern EM/EO Order of Battle	Specialized Tactical Aids





\* Either Numerical model values or measured values may be used , or both

Figure 1. Simplified flow diagram of the boundary layer model showing possible configurations of input information, interrelation between atmospheric and oceanic models, model outputs, and tactical models which use these outputs.

The predicted meteorological properties that are necessary to the above features and which are available from the NPS boundary layer model appear in the second column from the RHS in Figure 1 and are:

Inversion height and jump magnitudes:

The height of the inversion defines the depth of the marine boundary layer. This is also the elevation where electromagnetic trapping occurs. The index of refraction gradient governs the path curvature and the gradient depends on the changes (jumps) in temperature and water vapor in the inversion. The model outputs the index of refraction profile (in M units) for use in the IREPS program. The boundary layer depth also defines the region through which materials released within the layer are dispersed, a quantity which is needed for dispersion models. For example, aerosols generated at the sea surface are trapped within this layer, which impacts on optical extinction.

Boundary layer well mixed properties:

The equivalent potential temperature and total water mixing ratio (measures of temperature and moisture) are basic boundary layer properties that are used for all calculations within the model. They are also needed for all of the propagation models and are available as outputs.

Aerosol loading, extinction:

The aerosol equilibrium size distribution as a function of height is calculated on the basis of the ambient relative humidity and wind speed.

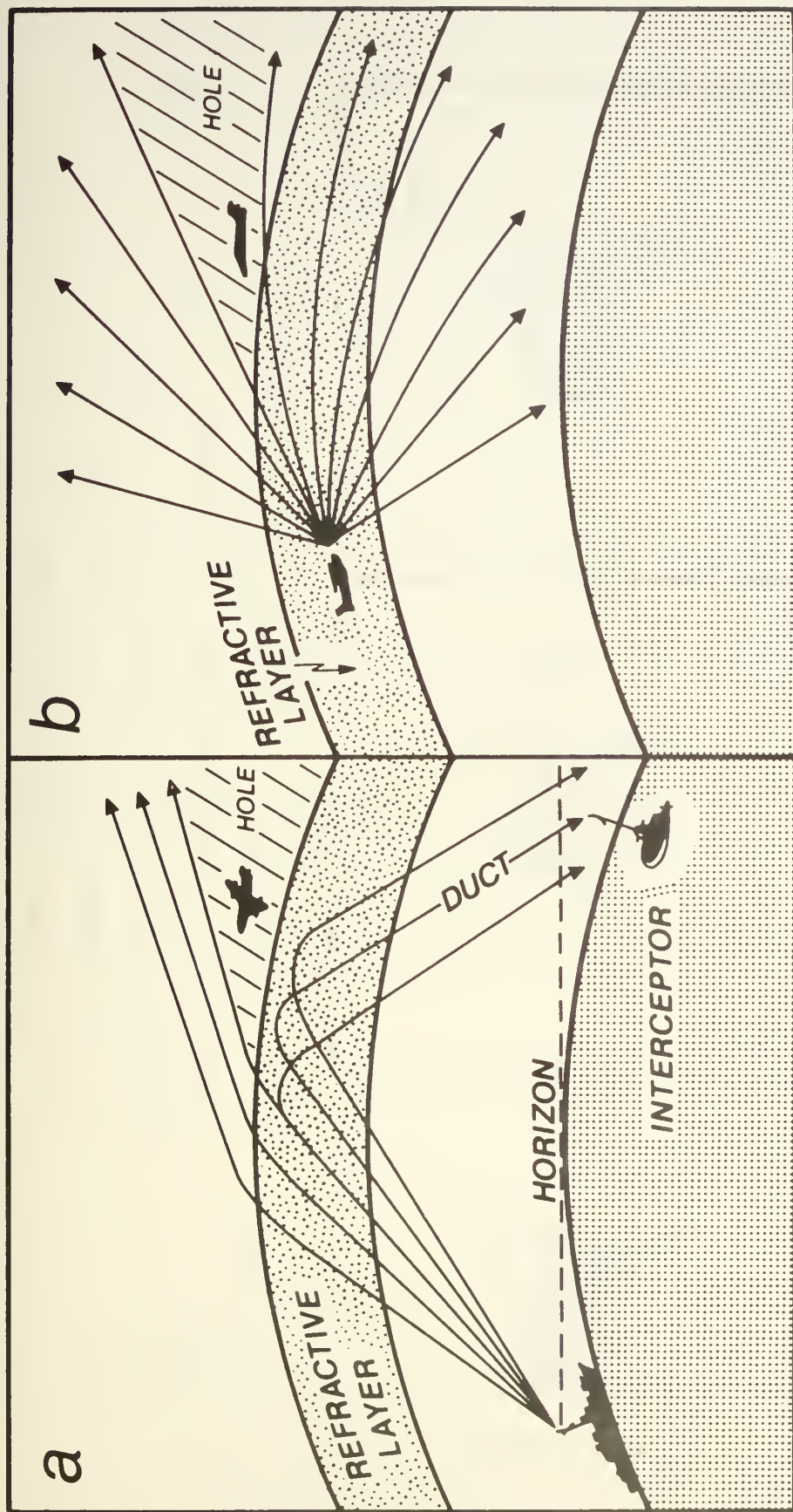


Figure 2. Examples of extended ranges and holes for EM ducts for

(a) surface-based duct and a shipboard air-search radar and

(b) elevated duct and an airborne early-warning radar

(from Hitney, 1979).



Figure 3. Computer simulated image of remotely piloted vehicle (RPV) as viewed with 8-12  $\mu\text{m}$  IR sensor (range 2 km, visibility 15 km, threshold 4.5 nW) through atmosphere with  $C_n^2$  values of (a) 0 (no turbulence), (b)  $3.7 \times 10^{-15} \text{ m}^{-2/3}$  and (c)  $1.0 \times 10^{-14} \text{ m}^{-2/3}$  (from Kearns and Walter, 1978).

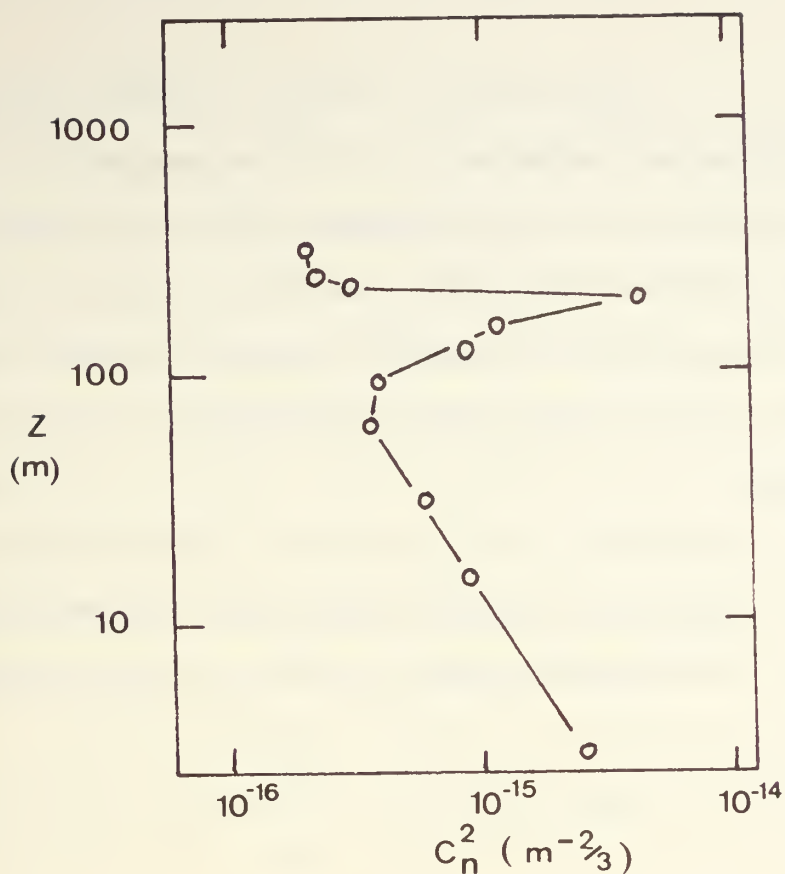


Figure 4. Measured variation of  $C_n^2$  with height. Data were obtained during the CEWCUM-76 experiment, 5 Oct 76.

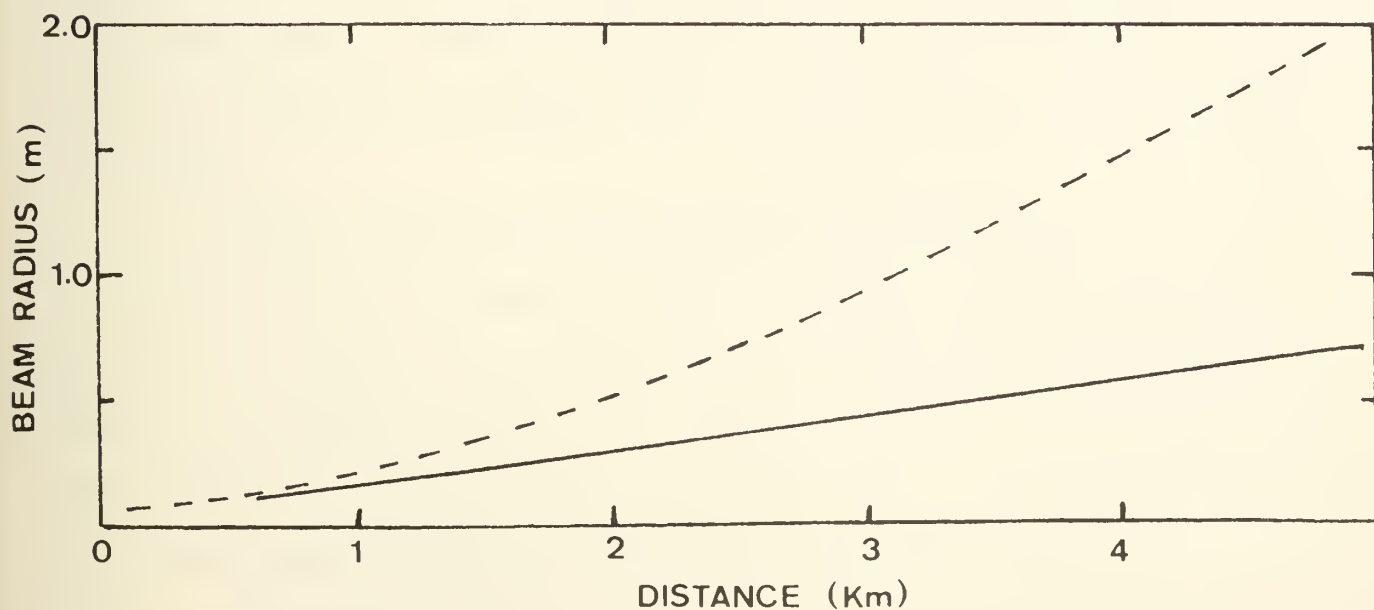


Figure 5. Variation of laser beam radius with distance for  $C_n^2$  levels of  $6.5 \times 10^{-15} \text{ m}^{-2/3}$  (solid line) and  $6.5 \times 10^{-13} \text{ m}^{-2/3}$  (dashed line).

### Fluxes:

The fluxes of momentum, heat and water vapor and the attendant turbulence intensities are all possible output parameters. The surface layer fluxes are needed to calculate evaporation duct properties. Turbulence intensities through the boundary layer are needed to calculate optical scintillation, wave front distortion and slant path propagation properties.

### Fog and cloud prediction:

An integral part of the model is the calculation of the vertical height at which condensation will occur, which is needed to determine the correct radiation balance. Thus fog/cloud prediction is a natural consequence of the model.



### 3. ATMOSPHERIC BOUNDARY LAYER MODEL CONSIDERATIONS

The marine atmospheric boundary layer (MABL) is coupled both to the overlying atmosphere and to the ocean below. Thus, if a model is to be successful, it must include large scale atmospheric processes, such as subsidence and advection, and oceanic processes which control the sea surface temperature.

To produce a tactically useful MABL model one must consider the operational environment in which it will be applied in addition to meteorological factors. Specifically,

#### a. Measurement of local meteorological parameters:

Radiosondes are normally released only once or twice a day. This information is used to determine atmospheric conditions for the day. If conditions are changing appreciably it might be necessary to launch another radiosonde balloon to provide updated input information to the model.

#### b. Determination of large scale parameters:

In the absence of data from large scale models, a single ship or station must be able to calculate synoptic scale forcing, e.g. subsidence, from local measurements. Several methods are available to determine vertical motion from radiosonde soundings, either from one station or multiple stations in a region.

#### c. Numerical prediction of local meteorological parameters:

Decisions must be made in formulating a model regarding which parameters will be predicted by the model and which ones should be input as forecasts to the model initially. For example, surface layer winds might come from another source and be input to the model when it is initialized, but the mixed layer temperature would be predicted by the model itself.

d. Possible alternative data sources:

1) Ocean models: The atmospheric and oceanic boundary layers are linked through the sea surface temperature (SST) which affects the surface fluxes of heat and moisture. An alternative to measuring the SST would be to predict it with an oceanic boundary layer model coupled to the MABL model.

2) Climatology: In the absence of other information, climatological inputs could be used for the model to provide the most probable boundary layer properties. Climatologies are very incomplete at this time, but should be more useful in the future.

3) Satellites: Satellite imagery might provide large scale information such as SST patterns. Much work is being done on extracting information from satellite images, and their value, especially in data sparse regions, is improving with time.

e. Output of information in the proper format:

If the output from a MABL model is to be used in tactical assessment programs it must be matched to the format required by them. The specific measure of each quantity (e.g. specific humidity or relative humidity for moisture) and the units required by the tactical assessment program need to be determined.

The flow diagram in Figure 1 is for a temporal assessment of the environment. (A spatial model would be more complicated than Figure 1 shows since it requires a Lagrangian approach, special inputs of the horizontal variation parameter, and a self consistency closure scheme.) Aspects of this scheme warranting further description are:

a. The atmospheric and oceanic models are considered separate entities; they are linked through the SST which is predicted in the oceanic model using output from the atmospheric model.

b. The propagation models use meteorological parameters as inputs and calculate propagation behavior. Most of these models do not calculate system performance directly but parameters related to the performance. The development of tactical aides that can be used directly in the field is underway. Description of these efforts is beyond the scope of this report.

c. The dynamics of the boundary layer are very sensitive to small changes in the meteorological parameters. A sensitivity analysis is needed to determine the accuracy with which these parameters should be specified. This will impact on measurement systems and techniques and on the design of synoptic scale numerical models.

#### 4. MODELING THE BOUNDARY LAYER

From a local assessment perspective, consider an idealization of the oceanic-atmospheric system. The air-sea interface is bordered by oceanic and atmospheric turbulent mixed layers (boundary layers) which are effectively insulated from the bulk ocean and free atmospheric regions. The primary sources of the turbulence within the atmospheric (oceanic) layers are the velocity (current) and buoyancy (density) gradients near the interface. Even under conditions where the water is slightly cooler than the air, buoyancy forced velocity fluctuations within the atmospheric layer can be quite large and mix the entire MABL from the surface to the inversion. The large vertical mixing yields constant (well-mixed) wind, temperature and humidity profiles above the surface. At the top of the atmospheric mixed layer there is a thin transition region (inversion), above it the free atmosphere, which is insulated from surface influence by the inversion. Idealizations of profiles of measures of moisture and temperature for this situation are shown in Figure 6.

The well-mixed nature enables prediction of MABL evolution to be based solely on fluxes at the two boundaries of the layer (inversion and sea surface) and on the large scale vertical velocity and advection. This is the basis of recent model formulations by Deardorff (1976) and Stage and Businger (1981) among others. Fluxes at both boundaries are due to buoyant and mechanically generated turbulence. The linear height variations of the fluxes of the well mixed properties allow one to relate fluxes at the inversion to the more readily determined surface layer fluxes and general cloud features. Approaches exist for estimating synoptic scale forcing from single station measurements<sup>\*</sup> but further efforts are required to achieve the accuracies required in MABL predictions.

---

<sup>\*</sup>This topic will be discussed in a forthcoming report on single station assessment.

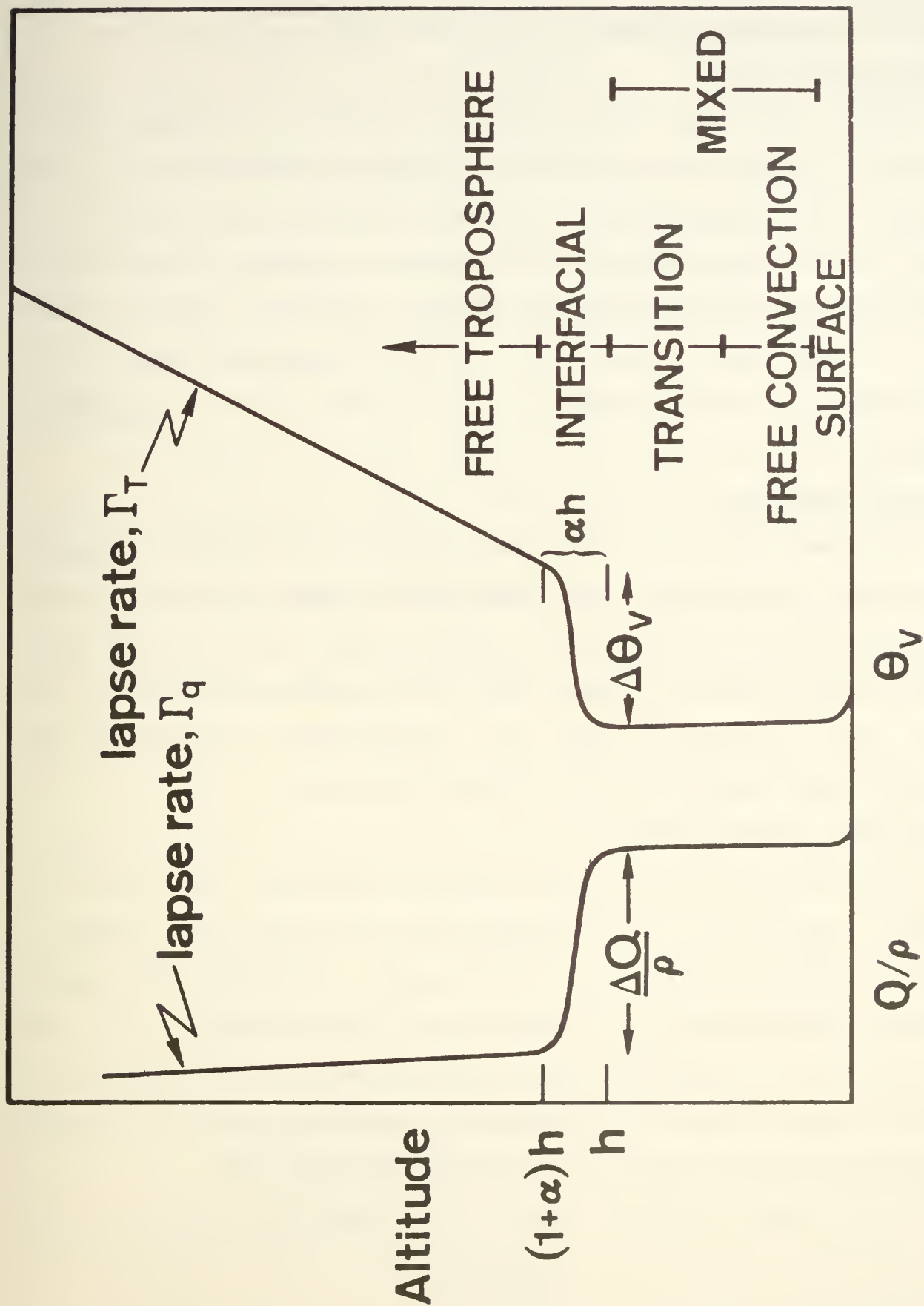


Figure 6. Idealized profiles of virtual potential temperature,  $\theta_v$ , and water vapor mixing ratio,  $Q$ , in a mixed-layer atmosphere.



Physical processes in the atmosphere that control the properties of the MABL can be grouped as follows:

#### Synoptic Scale Forcing

Synoptic scale mean vertical motion and advection are external factors influencing boundary layer evolution. Advection brings new air into the locality being evaluated so that the evolution of the boundary layer at a point does not depend solely on local features. Subsidence brings warm dry air from above, and will decrease the boundary layer height. These processes vary over time scales on the order of a day, changing as the synoptic situation changes. A frontal passage could lead to rapid changes in the synoptic forcing.

#### Surface Layer Fluxes

The surface layer is a region tens of meters deep immediately above the sea surface. In this layer wind, temperature and water vapor content change from surface to well-mixed values. Turbulent mixing in this layer is generated by wind shear and buoyancy. Due to the gradients, momentum, heat and water vapor are transported upward into the mixed layer. The surface layer thereby acts as a source region for the well-mixed layer.

#### Entrainment and the Inversion

The inversion is a region of wind shear and temperature and moisture gradients. Thus, it acts in much the same manner as the surface layer, being a region of important fluxes for the boundary layer. Turbulence erodes the inversion, mixing the warm dry air into the cool moist marine air. This flux process is called entrainment. Entrainment will warm and dry the marine air and will cause an increase in the boundary layer depth. It will also increase the boundary layer wind speed, if there are higher winds aloft.



## Radiation

Several radiative heating and cooling processes are operative:

- a. heating of the air by solar radiation,
- b. heating of the ocean by solar radiation,
- c. cooling of the sea surface by long wave radiation,
- d. cooling of the cloud top by long wave radiation,
- e. heating of the cloud region by solar radiation,
- f. exchange of long wave radiative energy between the sea surface and the cloud bottom.

## Condensation

Cloud formation will take place if the lifting condensation level is within the mixing layer, that is, if it is below the inversion. This is an important modeling consideration since the radiation balance depends so strongly on the presence or absence of clouds. The model predicts the inversion height and the lifting condensation level so that a fog/stratus forecast is a natural consequence. This allows the predictive model to branch between clear sky and cloud topped cases.

The computational flow of the NPS model which incorporates the above physical processes is illustrated in Fig. 7. The initialization is based on radiosonde information, identical to that required by IREPS, at the beginning of the forecast period and the specification must be made for the synoptic scale subsidence, surface layer wind and sea surface temperature during the forecast period. Gleason (1982) has described and evaluated our procedures for estimating subsidence from single station data. Reformulation efforts are now being conducted which should allow the prediction of the surface layer wind, given a geostrophic wind forecast, and the prediction of sea surface temperature based on forming an initial upper ocean layer.

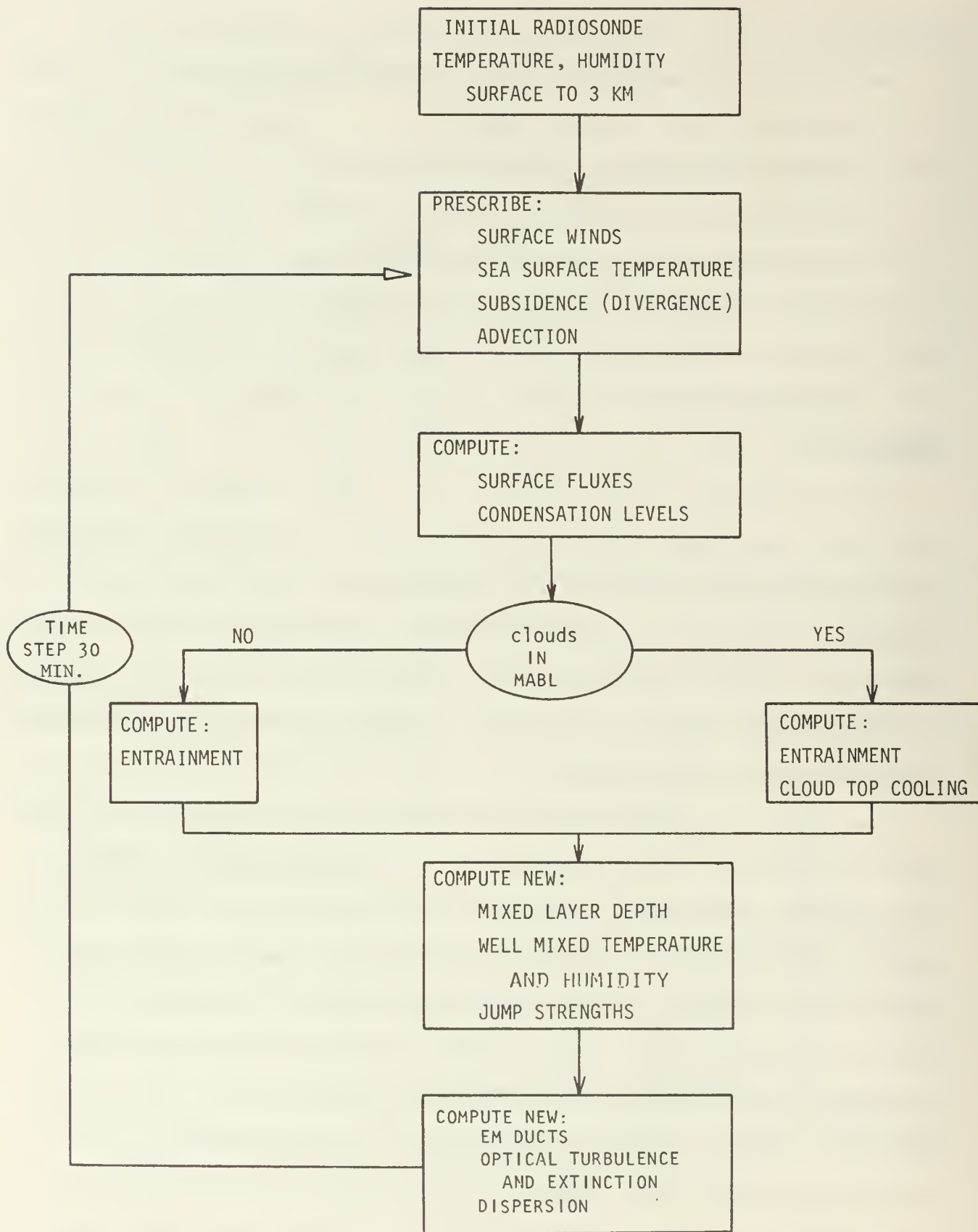


Figure 7. Schematic of input, prescription and computing steps in MABL prediction.

The predicted gradients are the mixed layer depth, temperature and humidity and the jump strength of the matter at the inversion. The predicted temperature and humidity are used to compute the surface fluxes and the cloud base, if any. The surface fluxes and cloud conditions determine the entrainment calculations. These differ for clear and cloudy skies and also for stable and unstable stratification in the surface. Parameters deferring EM/E0 propagation properties of the boundary layer are calculated from the values and distribution of predicted and specified quantities.

A 30 minute time step is used in the prediction calculation and it was based on representative mixing times for the MABL (Schacher et al, 1982). Running time for a 30 hour forecast on a HP 9845 computer is 10-12 minutes. Different running times arise for clear and cloudy sky periods because of the very extensive radiation calculation in the latter.

## 5. MODEL VALIDATION

Validation of the NPS integrated model approach is being done for many scenarios with data sets gathered in the Pacific, Atlantic and Indian Oceans. The results show that the technique is indeed a viable one, but these results must be considered preliminary in nature. The data were obtained on shipboard and would normally be available to the meteorology office on a Navy ship: wind speed, air temperature, sea surface temperature, humidity and radiosonde information. Acoustic sounder results were also available in some of the examined cases, but are not needed to run the model.

### a. Data Set

The data to be presented here were obtained during the Cooperative Experiment on West Coast Oceanography and Meteorology (CEWCOM-78) conducted west of San Nicolas Island, CA during May of 1978. Observations of both oceanic and atmospheric mixed layers were made from the R/V ACANIA and radiosonde observations were also taken at surrounding shore stations. The data to be shown are from a 48-hour period, 5/19/0500 to 5/21/0500 PST, when the R/V ACANIA was cruising slowly (2-3 knots) into the wind, returning to a reference point approximately every 12 hours. The general location of the R/V ACANIA during the 5/19 to 5/22 period and locations of surrounding shoreline radiosonde sites appear in Figure 8.

The period was one of steady onshore flow caused by the combined effects of intensification of the Eastern Pacific High and the persistence of the Mexican thermal low. The only apparent change in synoptic scale forcing during the period was an increase in the offshore pressure gradient. Such a synoptic change would have been predicted by the geophysics officer knowing that the high was intensifying. Satellite imagery showed increasing uniform stratus coverage (thin to heavy) during the period with a cellular (broken)

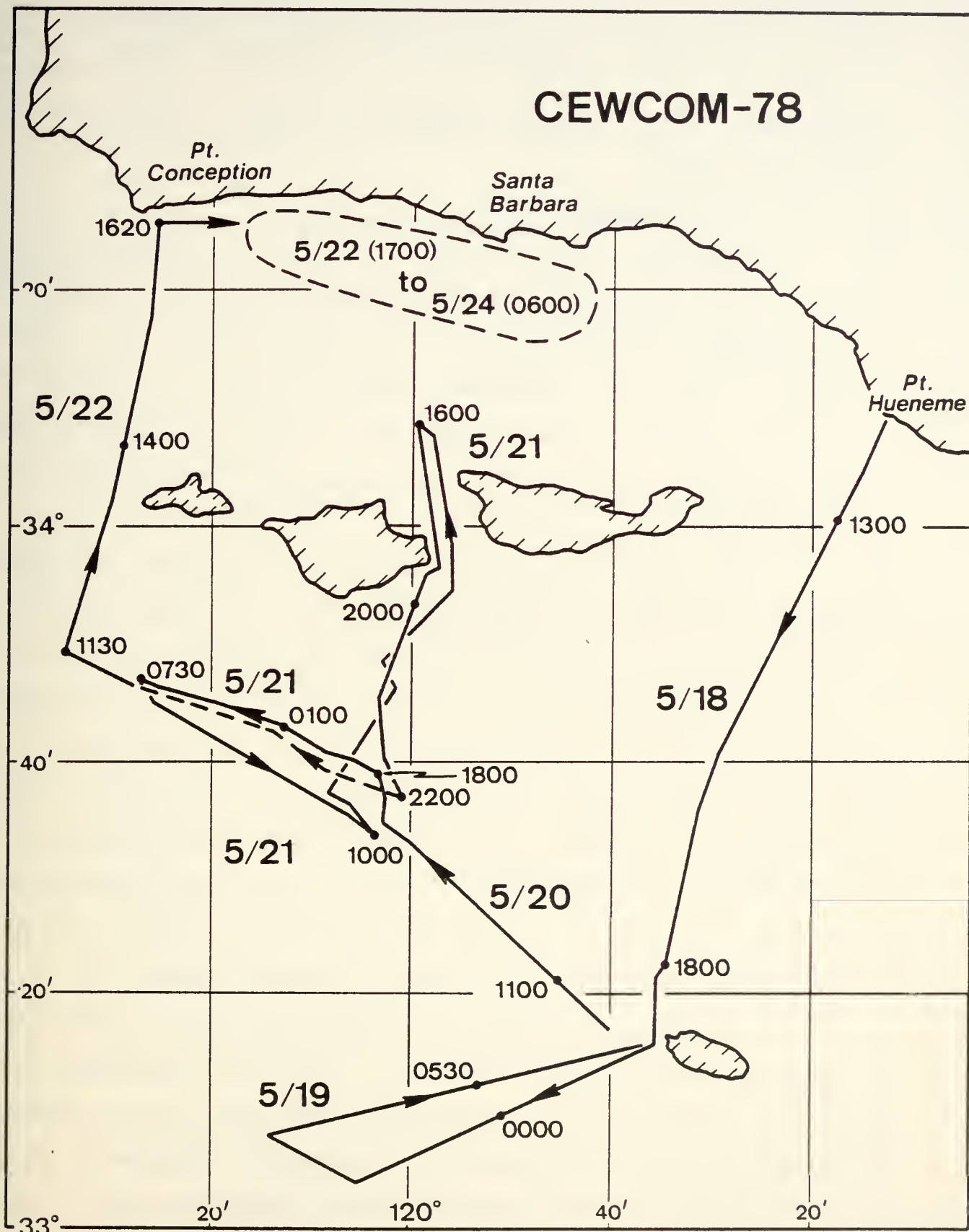


Figure 3. Track of P/V ACANIA and location of onshore radioscene sites during CEWCOM-78. The general location of the P/V ACANIA during the 19-21 May period is indicated by the hatched area N-77 of San Nicolas Island (SNL).



coverage occurring late on the 21st. The increase in cloud coverage is predicted by the model. We believe MABL evolutions were primarily determined by subsidence, surface fluxes, entrainment at the inversion, and cloud influenced radiative transfer.

b. Observed Changes

Observations during the 19-21 May period are presented in Figure 9. The half hour average values of wind, temperature and humidity measured aboard the R/V ACANIA are shown in 9c and d. The acoustic sounder trace from the R/V ACANIA is given in 9b. Atmospheric soundings are shown in 9a and are composites from the ship and land stations. Both slow and rapid changes in boundary layer properties which occurred were tactically significant, [as will be demonstrated].

The coupled variations of boundary layer parameters are apparent by examining the evolution on 5/20. During that day: 1) the MABL depth increased from 300 m to 500 m, 2) the wind speed increased from 5 to 10 m/sec, 3) the air temperature decreased from 15 to 13°C, 4) the sea surface temperature increased from 11 to 13°C, then went down to 12°C in the last five hours. Changes in the parameters indicate that the depth of the boundary layer was influenced by entrainment. Air entrained from above would be warmer, drier, and have increased momentum due to the higher wind speed above the inversion. This would lead to an increase in temperature, a decrease in relative humidity, and an increase in wind speed as is shown in Figure 9.

Possible coupling between the atmosphere and ocean is seen in the response of the SST to the increased wind speed. The wind caused increased mixing in the upper layer of the ocean, lowering the surface temperature by mixing in cooler water from below. The ocean mixed layer deepening was evident in bathythermography records obtained from the R/V ACANIA. The ocean



mixed layer deepened from 10 meters on 20 May to 50 meters on 21 May. Late on the 20th the air responded to the decreasing SST, decreasing  $1^{\circ}\text{C}$  in three hours.

An example of the the tactically relevant changes in the boundary layer is shown in Figure 10 with respect to the modified refractivity,  $M$ , for four different times. Changes of  $M$  profiles over the three day period of the experiment were significant. The vertical dotted lines delineate the duct regions. At 5/19/1700 a surface based duct extended to 300 m. As the boundary layer evolved the duct became elevated, and at 5/21/0500 had a base at 400 m and a top at 700 m.

### c. Model Predictions

The NPS boundary layer model has outputs in two basic formats: predicted time histories and predicted profiles of significant parameters. Two 24-hour model forecasts for the validation period are shown in Figures 11a and 12. Overlays of measured and predicted profiles of  $\theta$ ,  $q$ , and  $M$  are shown in Figure 11. The time histories in Figure 11 also show measured values of the various quantities, and are computed in half-hour time steps. The model was re-initialized at the end of the first 24-hour period, conforming to the procedure that would be used during operational conditions. Overlays of measured and predicted values of  $z_i$ ,  $z_{lc}$ , and  $z_e$  (evaporation duct), and surface layer values of  $C_n^2$  and  $\beta$  are shown in Figure 12.

The most significant conclusions that can be drawn from comparisons of model predictions and observations are as follows:

1) (Figure 11a) The mixed layer values of potential temperature ( $\theta$ ) and water vapor mixing ratio ( $q$ ) were predicted quite well. Values of potential temperature, determined by averaging data from several stations in the area, were predicted to within  $0.3^{\circ}\text{C}$  in the first 24 hour

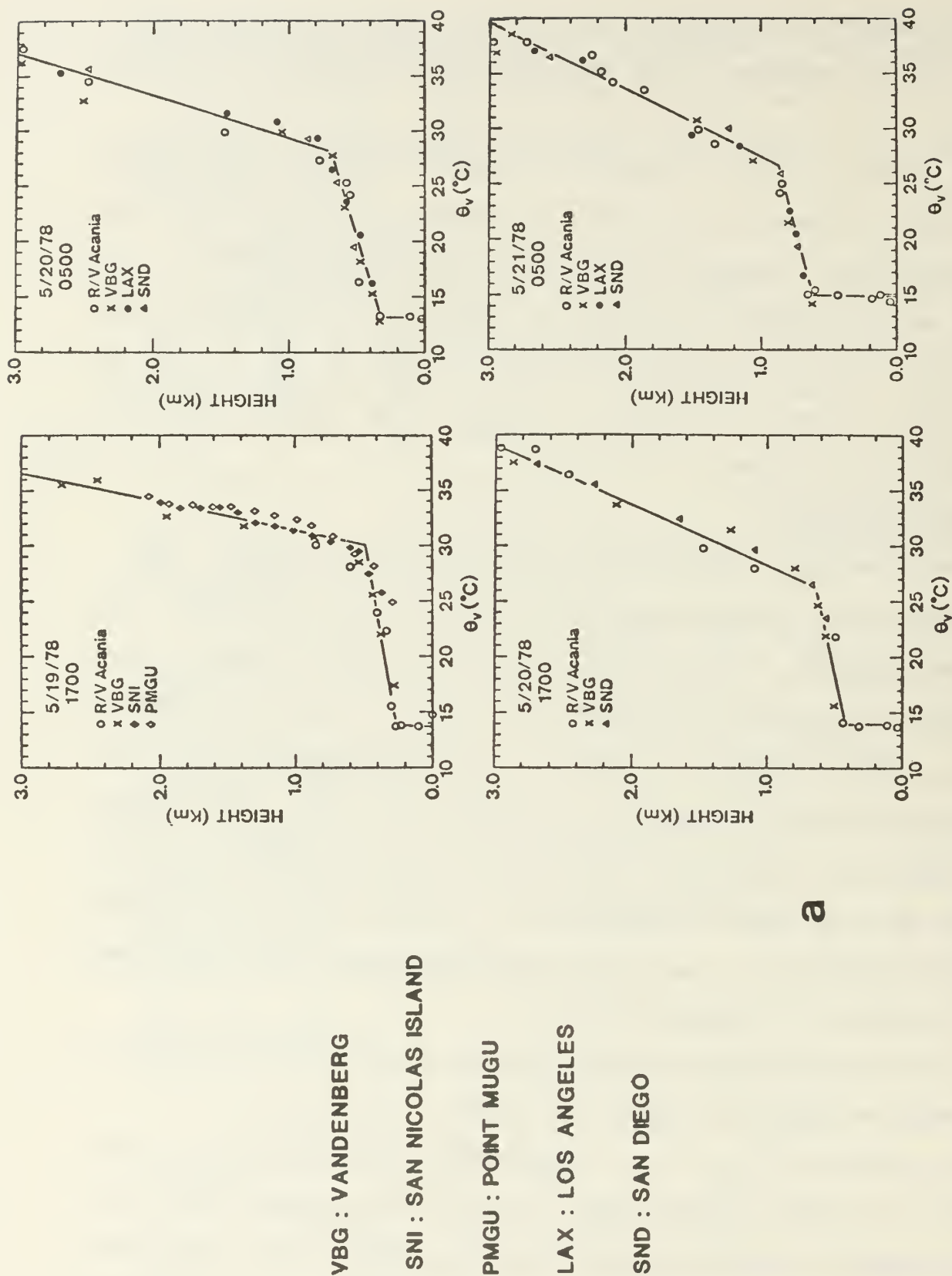
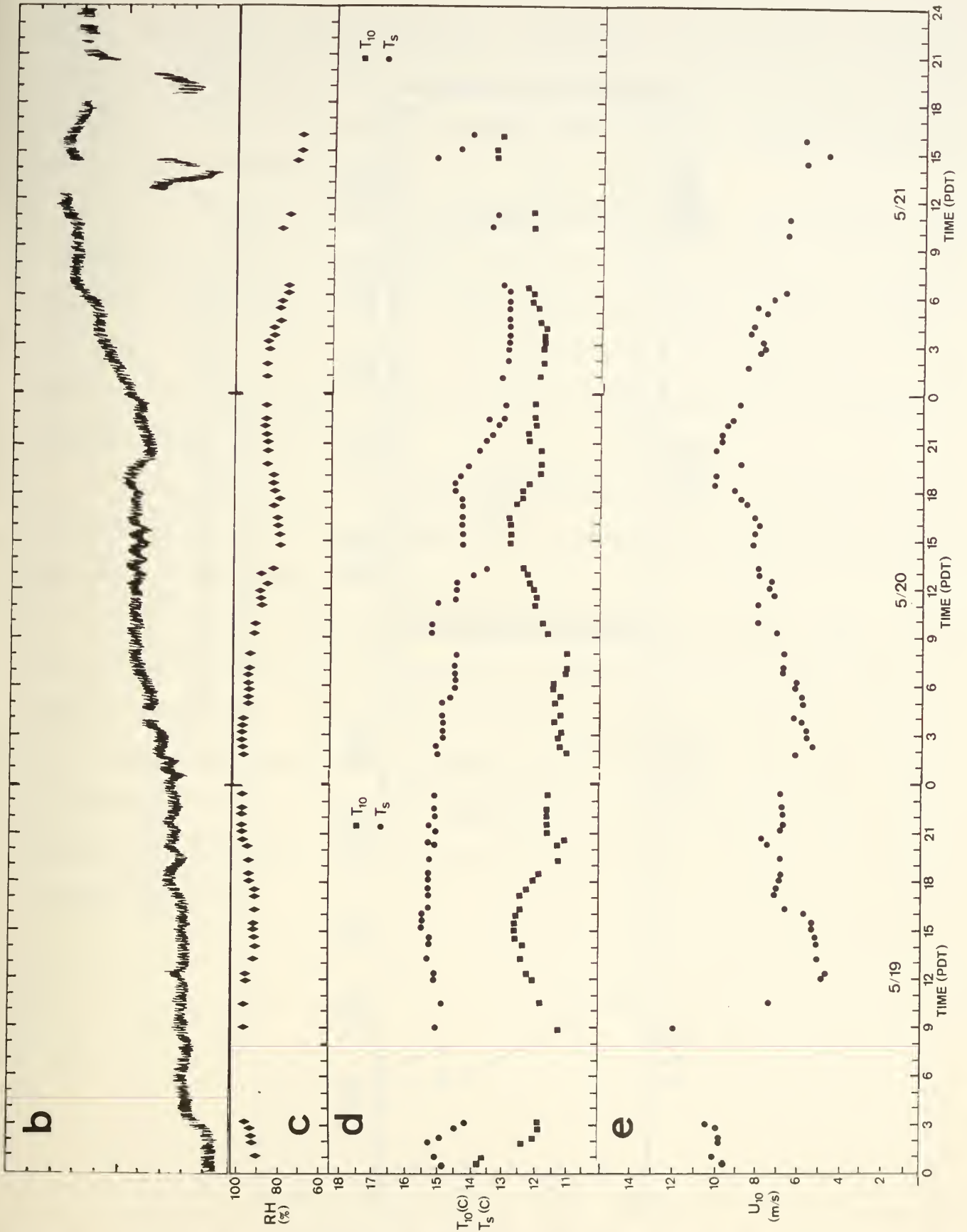


Figure 9. Atmospheric and oceanic mixed-layer observations during CEWCOM-78; (a) potential temperature composite profiles, (b) acoustic sounder record, (c) 10 meter relative humidity, (d) 10 meter and sea surface temperatures, (e) 10 meter wind speed. All data except the profiles indicated in (a) were obtained from the R/V Acania.



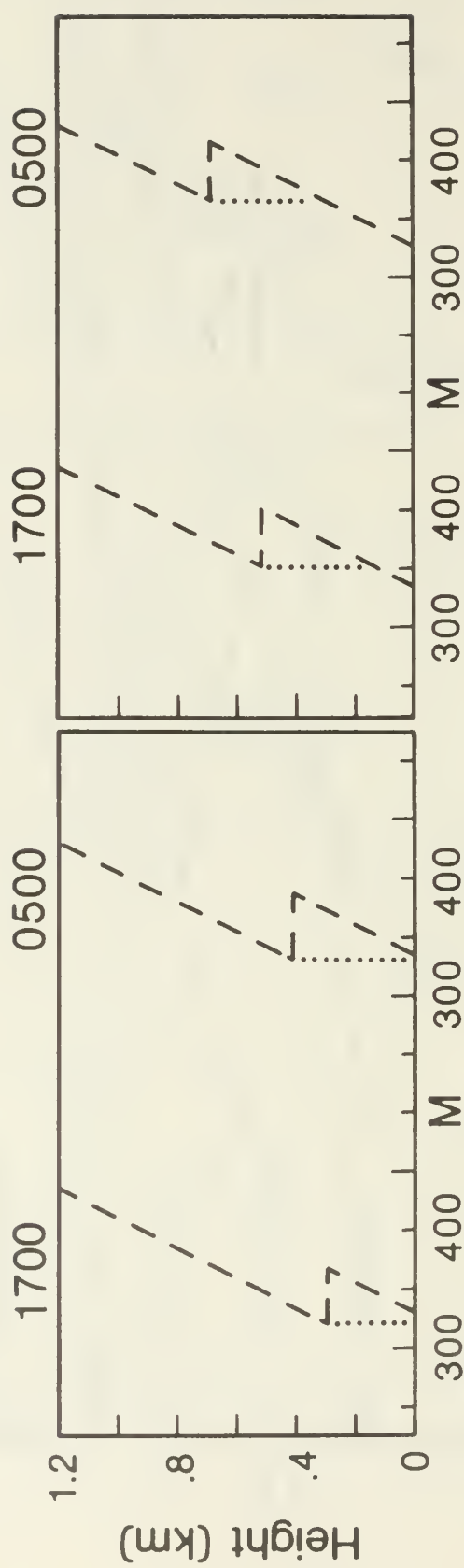


Figure 10. Observed profiles of the modified refractivity, M. Data were obtained at the approximate times indicated. The dotted line shows the boundary of the radar duct.

period and  $1.4^{\circ}\text{C}$  in the second period. During the first 24 hours the mixing ratio was predicted to within 0.9 g/kg; it was predicted to within 0.7 g/kg in the second 24 hours. These are the basic meteorological parameters on which the tactical parameters depend.

2) (Figures 11b, 12a) The height of the boundary layer and hence the height of the duct were predicted to within 14 m after 12 hours in the first period and within 58 m after 12 hours in the second period. After 24 hours the errors in the first and last period were 68 and 75 m respectively. The duct was accurately predicted to rise from a surface base to an elevated one between 0500 and 1700 on 20 May.

3) (Figure 12a) The model predicted the lifting condensation level to be below the top of the boundary layer, thus predicting clouds but not fog for the full period as was observed.

4) (Figures 12c and d) The model captures the surface layer values in  $C_n^2$  and  $\beta$  quite well, in addition to correctly predicting the trends in both 24 hour periods. The agreement arises in part because both of these are quite dependent on quantities which were prescribed with the observed values.  $C_n^2$  depends on the predicted air temperature and the prescribed sea surface temperature.  $\beta$  depends on the predicted relative humidity and the prescribed surface wind.

Figure 11. Observed and predicted MABL profiles for the 5/19/0500 to 5/21/0500 CEWCOM-78 period including (a)  $Q$  ( $\text{gm}^{-3}$ ) and  $\theta$  ( $^{\circ}\text{C}$ ), (b)  $M$ , (c)  $C_n^2$  ( $\text{m}^{-2/3}$ ), and (d) total extinction coefficient,  $\beta$  ( $\text{km}^{-1}$ ). Solid lines correspond to observations and dashed lines to model predicted values. The observed values were calculated from the meteorological parameters measured at the times indicated.



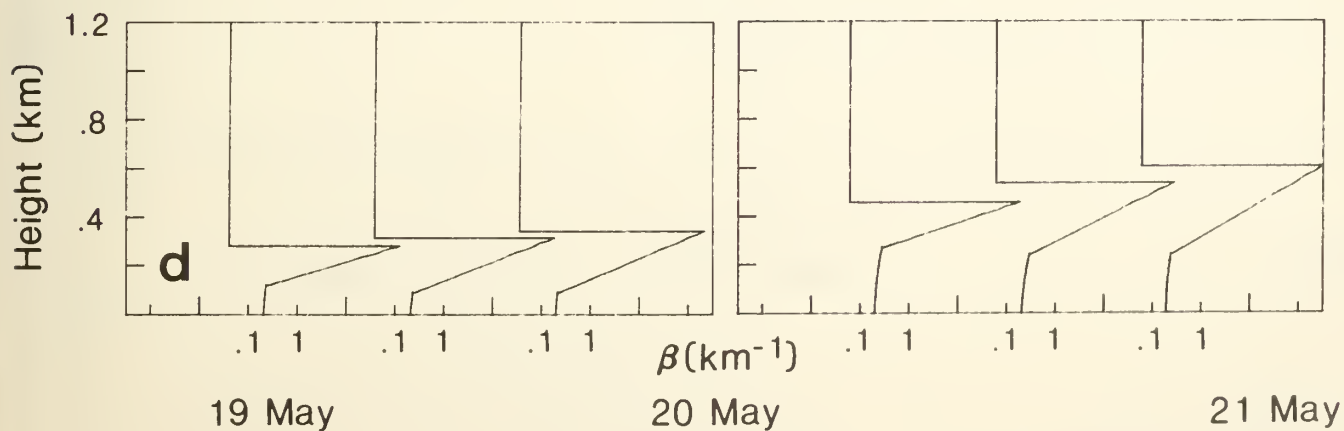
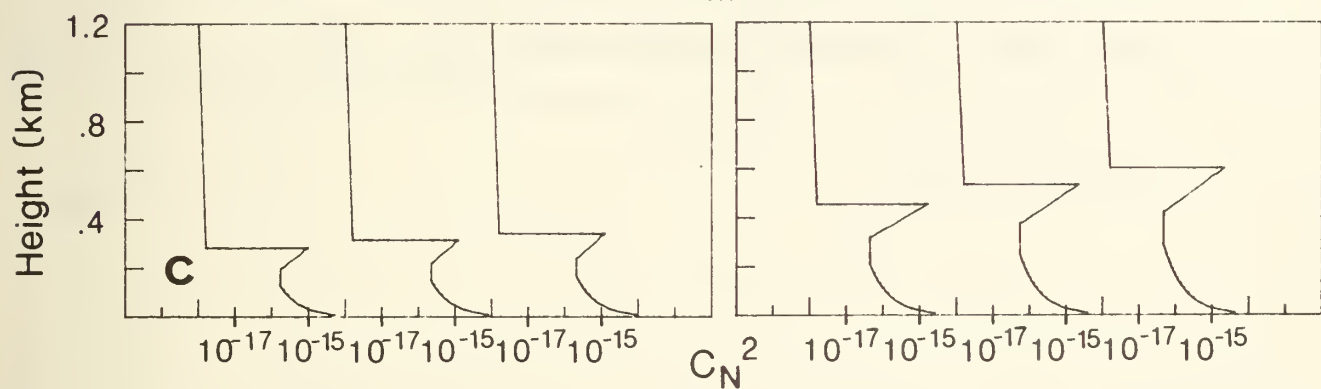
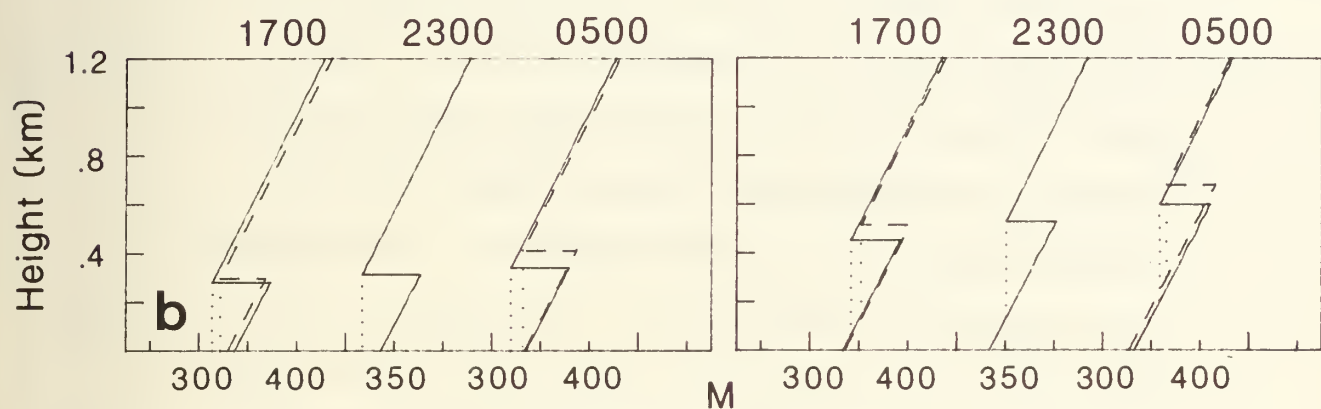
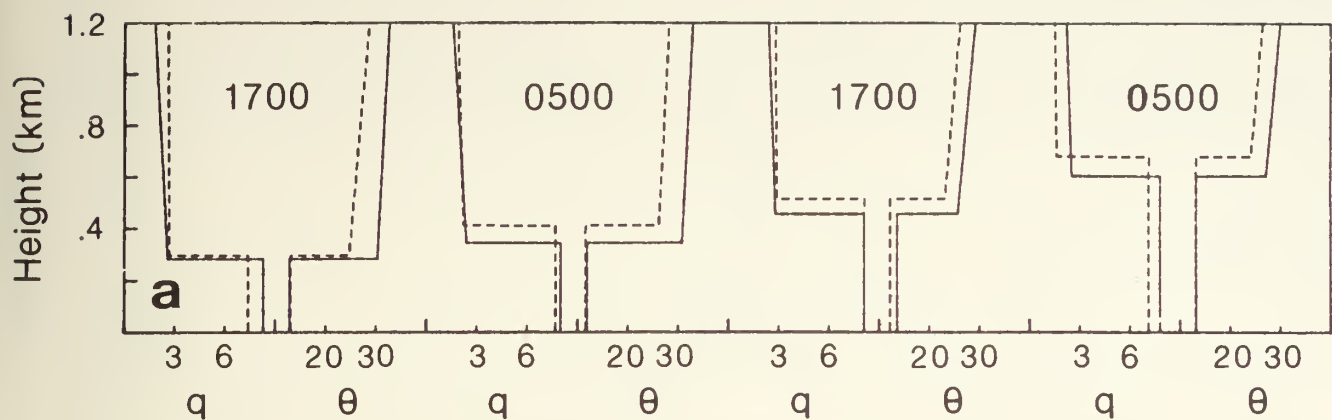
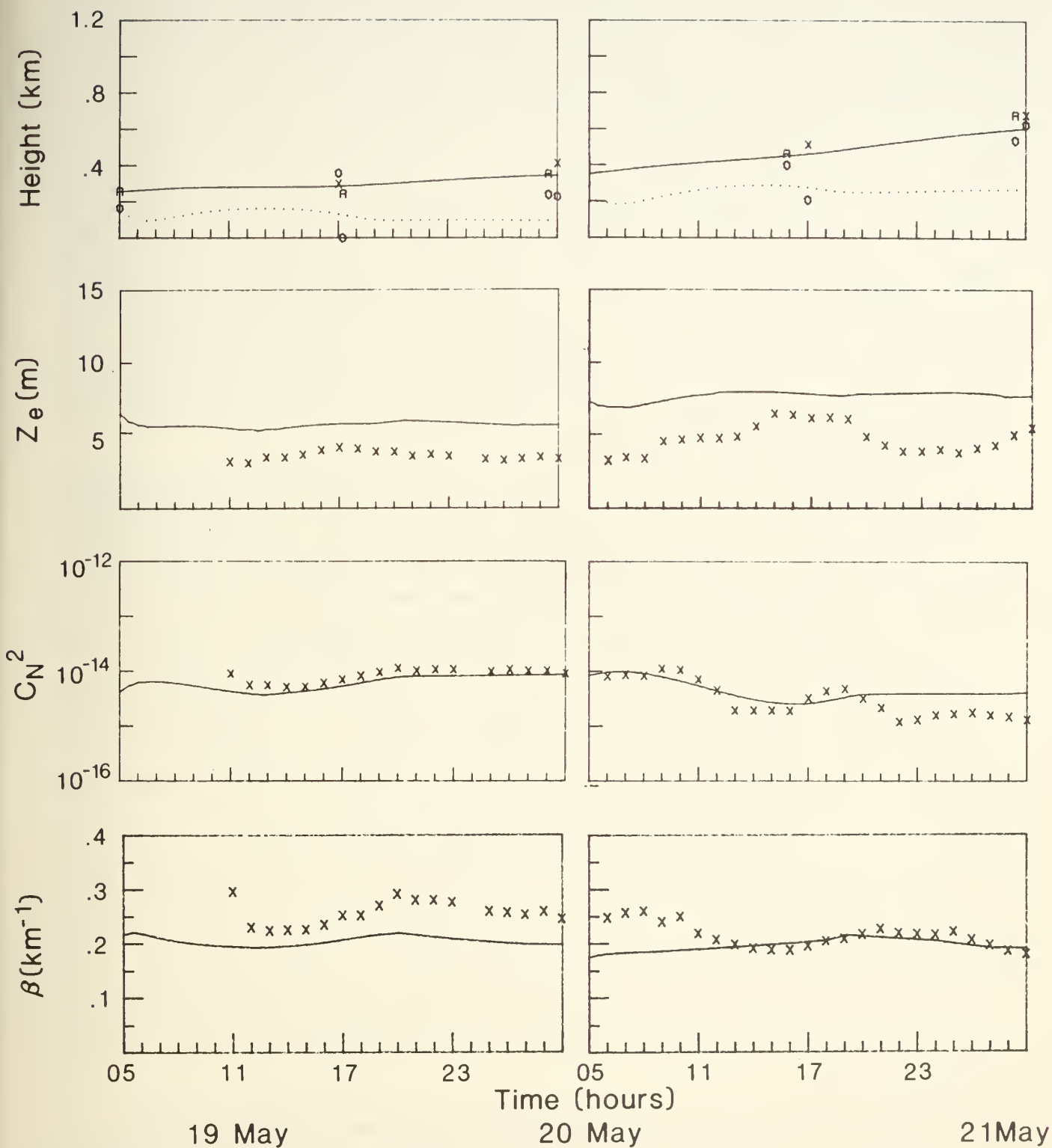


Figure 12. Observed and predicted surface layer values for the 5/19/0500 to 5/21/0500 CEWCUM-78 period: (a) inversion height ( $Z_i$ ) (solid line) and lifting condensation level (LCL) (dotted line). The A's represent inversion height determined from radiosonde soundings taken on the R/V ACANIA, the X's are inversion heights from composite soundings. The O's represent corresponding observed LCL's. (b) evaporation duct depth,  $Z_e$  (m), (c)  $C_n^2$  ( $m^{-2/3}$ ), and (d) total (aerosol and water vapor) scattering extinction coefficient,  $\beta$  ( $km^{-1}$ ). In (b)-(d) X's are the observed and solid lines are the model predicted values.



## 6. CONCLUSIONS

We have presented a description of features of the marine atmospheric boundary layer (MABL) which influence the performance of systems dependent on electromagnetic and optical wave propagation. We believe the effects of atmospheric properties on such systems can be estimated given accurate measurements. However, the properties change in both time and space so predictive capabilities are necessary. We further believe that predictions should be based, as much as possible, on local observations, on synoptic scale forcing discernable by an aircraft carrier based geophysics officer and on calculations which can be made with a microcomputer such as those planned for the Tactical Environment Support System (TESS) used for the existing IREPS code for electromagnetic wave propagation.

We have presented a simplified slab model for predicting relevant changes of the MABL due to wind and buoyancy forced mixing and cloud radiative effects. It requires as input, temperature and humidity profiles from an initial radiosonde and prescription of sea surface temperatures, surface winds and subsidence for the forecast period. It predicts the temperature and humidity below the inversion, the inversion height, the magnitudes of the humidity and temperature jumps at the inversion and the lifting condensation level. From the above predicted and the prescribed meteorological properties, one can calculate the dimensions of elevated and surface based radar ducts, the intensities of optical turbulence and the magnitude of optical extinction due to molecular absorption and aerosol scattering. The latter depend on the empirical expressions relating aerosol size distributions to wind speed and relative humidity.

The NPS physical model, the initialization and the synoptic scale prescription were evaluated from a 48 hour period when a cloud topped MABL was

deepening from 250 to 750 meters. The conditions occurring were well documented on the basis of shipboard and surrounding island and shoreline observations. The most significant changes in conditions in the tactical environment were 1) an initial surface based radar duct became an elevated duct at end of the first 24 hours and remained elevated throughout the second 24 hour period; 2) an overcast to broken stratus layer persisted throughout the 48 hour period which did not lower to cause a fog episode and 3) the surface layer wind increased steadily from 5 to 10 m s<sup>-1</sup> during the first 24 hour period.

The model was run on a microcomputer, which is aboard all carriers, and predicted the first two tactical descriptions quite well. The surface based radar duct was predicted to become elevated by the end of the first 24 hours and remain elevated throughout the second 24 hours. The predicted and observed dimensions agreed reasonably well in view of uncertainties and averaging in the observed radiosonde data. This agreement in duct dimensions required accuracy in the prediction of the inversion height, jumps at the inversion and mixed layer temperature and humidities. The predicted lifting condensation level was always well below the predicted inversion height implying an overcast stratus layer with base ranging from 100 m during the first 24 hour period and lifting to 200 m during the second 24 hour period. The top of the layer corresponded to the predicted inversion height. Observed lifting condensation levels were always higher (factors of 2) than the predicted. The agreement on stratus cloud coverage, even though the bases were too low, required reasonably accurate predictions of the mixed layer temperature, humidity and depth (inversion height).

The wind speed increase, the third tactical description, was not a predicted property in the current model but was probably influenced by the



deepening of the layer. The model is being reformulated to include this prediction as well as to couple the model to an ocean mixed layer model. These reformulations will be important in achieving bonafide predictions of the other surface layer parameters: optical turbulence ( $C_n^2$ ), extinction ( $\beta$ ) and evaporation duct height ( $Z_e$ ).

We believe the demonstrated reasonable success from present modeling efforts in the prediction of the tactically significant features of the MABL is encouraging. This encouragement exists because it requires a computer and input which are available to a geophysics officer on a ship or at a shore facility. Several required areas of improvements and reformulations have been identified. They are:

- 1) improve single station estimates of synoptic scale subsidence and advection;
- 2) include surface layer wind prediction based on synoptic (geostrophic) wind;
- 3) couple MABL to ocean mixed layer model so that coincident evolutions are predicted and feedback occurs through sea surface temperature changes.

## References

- Deardorff, J. W., 1976: On the Entrainment Rate of a Stratocumulus-Topped Mixed Layer. Quart. J. R. Met. Soc., 102, 563-582.
- Fairall, C. W., K. L. Davidson and G. E. Schacher, 1981: A Review and Evaluation of Integrated Atmospheric Boundary-Layer Models for Maritime Applications. Tech. Rept. NPS-63-81-004, Naval Postgraduate School, Monterey, CA, 83 pp.
- Gleason, J. P., 1982: Single-Station Assessments of the Synoptic-Scale Forcing on the Marine Atmospheric Boundary Layer. Master's Thesis, Naval Postgraduate School, Monterey, CA, 52 pp.
- Hitney, H. V., 1979: Integrated Refractive Effects Prediction System (IREPS) and Environmental/Weapons Effects Prediction System (E/WEPS), Proceedings, Conference on Atmospheric Refractive Effects Assessment 23-25 January 1979, Naval Ocean Systems Center Technical Document, NOSC PD 260, 13-17.
- Ruggles, K. W., 1975: Environmental Support for Electro-Optics Systems. Fleet Numerical Weather Central Tech. Rept. 75-1, FNOC, Monterey, CA, 47 pp.
- Schacher, G. E., K. L. Davidson and C. W. Fairall, 1981: Atmospheric Marine Boundary Layer Convective Mixing Velocities in the California Coastal Region. Atmos. Environment, 16, 1183-1191.
- Stage, S. A. and J. A. Businger, 1981: A Model for Entrainment into a Cloud-Topped Marine Boundary Layer. Part I. J. Atmos. Sci., 38, 2213-2229.



# DISTRIBUTION LIST

	No. of Copies
1. Defense Technical Information Center Cameron Station Alexandria, Virginia 22314	2
2. Library, Code 0142 Naval Postgraduate School Monterey, California 93940	2
3. Dean of Research, Code 012 Naval Postgraduate School Monterey, California 93940	1
4. Professor J. Dyer, Code 61Dy Naval Postgraduate School Monterey, California 93940	1
5. Professor R. J. Renard, Code 63Rd Naval Postgraduate School Monterey, California 93940	1
6. Professor C.N.K. Mooers, Code 68Mr Naval Postgraduate School Monterey, California 93940	1
7. Professor K. L. Davidson, Code 63Ds Naval Postgraduate School Monterey, California 93940	10
8. Professor G. E. Schacher, Code 61Sq Naval Postgraduate School Monterey, California 93940	10
9. Assoc Prof R. W. Garwood, Code 68Gd Naval Postgraduate School Monterey, California 93940	1
10. Dr. C. W. Fairall BDM Corporation 1340 Munras Street Monterey, California 93940	10
11. Mr. Don Spiel BDM Corporation 1340 Munras Street Monterey, California 93940	2
12. Dr. A. Weinstein Director of Research Naval Environmental Prediction Research Facility Monterey, California 93940	1





13. CAPT K. Van Sickle 1  
Naval Environmental Prediction Research Facility  
Monterey, California 93940
14. Dr. A. Goroch 1  
Naval Environmental Prediction Research Facility  
Monterey, California 93940
15. Dr. Alex Shlanta, Code 3173 1  
Naval Weapons Center  
China Lake, California 93555
16. Dr. Barry Katz, Code R42 1  
Naval Surface Weapons Center  
White Oak Laboratory  
Silver Spring, Maryland 20362
17. Dr. J. H. Richter, Code 532 1  
Naval Ocean Systems Center  
San Diego, California 92152
18. Dr. Lothar Ruhnke, Code 8320 1  
Naval Research Laboratory  
Washington, D.C. 20375
19. Mr. Herb Hitney, Code 532 1  
Naval Ocean Systems Center  
San Diego, California 92152
20. Mr. Herb Hughes, Code 532 1  
Naval Ocean Systems Center  
San Diego, California 92152
21. Mr. Stuart Gatham, Code 8320 1  
Naval Research Laboratory  
Washington, DC 20375
22. LCDR Stan Grigsby, PMS-405 1  
Naval Sea Systems Command  
Washington, DC 20360
23. Dr. Steven Burke 1  
Naval Environmental Prediction Research Facility  
Monterey, California 93940
24. Mr. Sam Brand 1  
Naval Environmental Prediction Research Facility  
Monterey, California 93940

25. Mr. Paul Banas, Code 9220 1  
Naval Oceanographic Office  
NSTL Station, Mississippi 39522
26. Dr. Paul Moersdorf, Code 9220 1  
Naval Oceanographic Office  
NSTL Station, Mississippi 39522
27. LT Mark Schultz 1  
Naval Environmental Prediction Research Facility  
Monterey, California 93940
28. Mr. Ted Zuba, Code AIR-370 1  
Naval Air Systems Command  
Washington, DC 20360
29. Mr. Jay Rosenthal 1  
Geophysics Division  
Pacific Missile Range  
Point Mugu, California 93042
30. Dr. Michael J. Kraus 1  
AFGL/LYS  
Hanscom AFB, Massachusettes 01731
31. MAJ Bob Wright 1  
AWS/DOOE  
Scott AFB, Illinois 62225
32. MAJ Ed Kolczynski 1  
AWS/SYX  
Scott AFB, Illinois 62225
33. Mr. Joel S. Davis 1  
Defense Sciences Division  
Science Applications, Inc.  
1010 Woodman Drive, Suite 200  
Dayton, Ohio 45432
34. Mr. L. Biberman 1  
Institute for Defense Analysis  
400 Army Navy Drive  
Arlington, Virginia 22202
35. Dr. Richard Gomez 1  
DELAS-E0-M0  
Atmospheric Sciences Laboratory  
White Sands, New Mexico 88002
36. Dr. R. Fenn 1  
Air Force Geophysics Laboratory  
Hanscom AFB, Massachusetts 02173

37. Mr. Glen Spaulding, MAT 72 1  
Naval Material Command  
Washington, DC 20362
38. Dr. Paul Twitchell 1  
Office of Naval Research  
666 Summer Street  
Boston, Massachusetts 02210
39. CDR Thomas Callaham, Code N341 1  
Naval Oceanography Command  
NSTL Station, Mississippi 39529
40. CAPT Ronald Hughes, Commander 1  
Naval Oceanography Command  
NSTL Station, Mississippi 39529
41. CAPT Ernie Young, OP 952 1  
Oceanographer of the Navy  
Washington, DC 20360
42. Dr. Lowell Wilkens 1  
Naval Weapons Center  
China Lake, California 93553
43. Dr. Ed Monahan 1  
Department of Oceanography  
University College  
Galway, IRELAND
44. Mr. Walter Martin, Code 470 1  
Office of Naval Research  
800 N. Quincy Street, Rm 307  
Arlington, Virginia 22217
45. Dr. Gloria Patton 1  
Office of Naval Research  
1030 E. Green Street  
Pasadena, California 91106
46. Mr. Jim Hughes, Code 470 1  
Office of Naval Research  
800 N. Quincy Street  
Arlington, Virginia 22217
47. Dr. Warren Denner 1  
Science Applications, Inc.  
2999 Monterey-Salinas Hwy  
Monterey, California 93940
48. Mr. George Hanssen 1  
Science Applications, Inc.  
P.O. Box 1303  
1710 Goodrich Drive  
McLean, Virginia 22102

- |     |  |   |
|-----|--|---|
| 49. | Dr. Lou Goodman, Code 481<br>Office of Naval Research<br>Physical Oceanography<br>NSTL Station, Mississippi 39529      | 1 |
| 50. | CDR S. G. Colgan, Code 420B<br>Office of Naval Research<br>800 N. Quincy Street<br>Arlington, Virginia 22217           | 1 |
| 51. | Dr. John A. Cooney<br>Dept of Physics and Atmospheric Science<br>Drexel University<br>Philadelphia, Pennsylvania 19104 | 1 |
| 52. | Mr. Thomas Rappolt<br>Energy Resources Company, Inc.<br>3344 N. Torrey Pines Court<br>La Jolla, California 92037       | 1 |
| 53. | MAJ Gary G. Worley<br>Air Force Engineering and Services Center<br>Tyndall AFB, Florida 32403                          | 1 |
| 54. | Mrs. Patricia Boyle, Code 63Bp<br>Naval Postgraduate School<br>Monterey, California 93940                              | 2 |
| 55. | Mr. Peter Guest, Code 63Ps<br>Naval Postgraduate School<br>Monterey, California 93940                                  | 2 |
| 56. | Lcdr D. A. Brower<br>USS SARATOGA (CV-60)<br>FPO New York 09501  | 2 |





DUDLEY KNOX LIBRARY



3 2768 00302449 8